Clean Fuel, Clean Energy Conversion Technology: Experimental and Numerical Investigation of Palm Oil Mill Effluent Biogas Flameless Combustion

Seyed Ehsan Hosseini,* Ghobad Bagheri, Mazlan Abdul Wahid, Aminuddin Saat

The combustion of effluent biogas from a palm oil mill is not feasible on a large scale because of its low calorific value (LCV). Therefore, the captured biogas is usually flared because of a lack of appropriate combustion technology. However, such biogas could be an excellent source of energy for combined heat and power (CHP) generation in palm oil mills. In this paper, the feasibility of using biogas from palm oil mills in flameless combustion systems is investigated. In computational fluid dynamic (CFD) modeling, a two-step reaction scheme is employed to simulate the eddy dissipation method (EDM). In such biogas flameless combustion, the temperature inside the chamber is uniform and hot spots are eliminated. The peak of the non-luminous flame volume and the maximum temperature uniformity occur under stoichiometric conditions when the concentration of oxygen in the oxidizer is 7%. In these conditions, as the concentration of oxygen in the oxidizer increases, the efficiency of palm oil mill effluent biogas flameless combustion increases. The maximum efficiency (around 61% in the experiment) is achieved when the percentage of oxygen in the oxidizer is 7%.

Contact information: High-Speed Reacting Flow Laboratory, Faculty of Mechanical Engineering Universiti Teknologi Malaysia, 81310 UTM Skudai, Johor, Malaysia;
* Corresponding author: seyed.ehsan.hosseini@gmail.com; Mazlan@fkm.utm.my

INTRODUCTION

The capture of biogas from wastewater effluent, municipal solid wastes (MSW), animal waste, and agricultural products has been developed throughout the world, not only to preserve the environment from toxic emissions, but also to generate heat and power (Al-Juhaimi *et al.* 2014). Palm oil, as one of the most well-known biofuel resources, has been developed widely in Southeast Asian countries such as Indonesia and Malaysia because of its environmentally friendly characteristics, which promise a clean alternative fuel (Dungani *et al.* 2013). Palm oil, which is approximately 28% of the total annual biofuel production, is the most widely used vegetable oil in the world (Hansen *et al.* 2012). However, sustainability of palm oil-based biodiesel production is under question as a result of generation of liquid effluent. Biogas released from palm oil mill effluent contains greenhouse gases that can endanger the environment, and such release has become the most important challenge in the palm oil production process. The negative effect of methane (CH_4) (one of the most important components of biogas) on the environment is 23 times more than carbon dioxide (CO_2). The percentage of CH_4 in collected biogas components is high enough to be considered a clean fuel. In palm oil mill effluent biogas, the amount of CH_4 is around 60%. Other impurities, such as 39% CO_2 and less than 1% hydrogen sulfide

(H_2S), hydrogen (H_2), nitrogen (N_2), and water vapor, are the main components that make up such biogas (Hosseini and Wahid 2013).

The calorific value of palm oil mill effluent biogas is approximately 22 MJ/m^3, which is lower than natural gas (NG), with 36 MJ/m^3. Thus, conventional combustion of pure palm oil mill effluent biogas encounters some problems. The percentage of CH_4 in biogas could be increased up to 90% by application of some advanced biogas upgrading technologies, such as membrane and cryogenic methods. However, the induced costs associated with these biogas purifications are very expensive. Therefore, new economic methods should be introduced to extract palm oil mill effluent biogas energy with some alternative pretreatments. Recently, flameless combustion has attracted attention because of its ability to intensify thermal efficiency while simultaneously reducing pollution. These characteristics make flameless combustion a unique technology, considering most other pollutant reduction techniques are associated with low thermal efficiency. Although the concept of fossil fuel flameless combustion has been extensively investigated experimentally and mathematically, biogas flameless combustion has received little attention.

In the production of one ton of crude palm oil (CPO); 2.5 tons of palm oil mill effluent is generated. Each ton of palm oil mill effluent is able to generate 28.13 m^3 of biogas. This means that by production of one ton of CPO, approximately 70 m^3 biogas could be captured (Hosseini and Abdul Wahid 2013). In a typical palm oil mill, with 200,000 tons of CPO production *per annum*, 14,000,000 m^3 of palm oil mill effluent biogas is generated per year. Because the associated biogas upgrading process is expensive and conventional combustion of the biogas is difficult because of its LCV; the captured biogas is usually flared. If the LCV of palm oil mill effluent biogas is considered, 5.95 kWh/m^3, and just 50% of this annual generated biogas is employed in CHP generation with flameless combustion (60% efficiency), approximately 24.9 MW of green electricity is available. This amount of power is ten times more than the electricity demand of the assumed palm oil mill. Because flameless combustion has not been employed seriously in palm oil mills, this paper tries to illustrate different aspects and capabilities of palm oil mill effluent biogas flameless combustion. In this experiment, a lab-scale flameless chamber is fueled by biogas collected from a palm oil mill in Malaysia with 70% CH_4 and 30% CO_2.

If palm oil mill effluent biogas is charged to the burner orifice at the pressure intended for feeding NG or LPG, the air to fuel ratio is not sufficient to generate a stable flame because of the high CO_2 content of biogas. Therefore, a second burner with a new control measurement system for biogas should be provided in parallel with the first. Some equipment should be employed in the switchover from NG or LPG to the biogas. Also, the corrosion factor of raw palm oil mill effluent biogas and the capability of the furnace fueled by LCV biogas should be taken into consideration to guarantee a stable flame. To reduce the corrosion phenomena associated with water vapor and H_2S, condensation should be prevented by maintaining the temperature above the dew point temperature. Therefore, the combustion chamber should be heated up by NG or LPG to achieve a higher operating temperature. Thus, application of a dual role burner in a conventional combustion system fueled by biogas is unavoidable. Complicated equipment and settings, as well as the low efficiency of the system, are the main barriers to biogas utilization development in the conventional combustion form (Bedoya *et al.* 2012).

Biogas Flameless Combustion

In the 1990s, flameless combustion emerged as a promising combustion technology characterized by a highly diluted and preheated oxidizer exceeding the auto-ignition temperature of the fuel. In the flameless combustion regime, fuel is burnt in a low-oxygen concentration environment without visible radiation from the flame. NO_x and soot formation are suppressed, and the level of noise is very low (Rebola *et al.* 2013). Although the temperatures of the preheated oxidizer in flameless combustion mode are higher than in conventional conditions, the reaction-controlling temperatures are lower than in traditional combustion because of the low oxygen concentration. High-momentum preheated air can be injected from the central part of the burner, which is surrounded by some low-momentum fuel jets. In the biogas flameless regime, biogas is mixed with a highly diluted and preheated oxidizer to distribute the reaction zone and mitigate the peak temperature. The elevated and uniform temperature distribution in the flameless combustor and low oxygen concentration circumstances lead the system to slower reaction rates and increase the effects of molecular diffusion on combustion characteristics (Gassoumi *et al.* 2009).

EXPERIMENTAL

Figure 1 depicts the experimental set-up schematically. The flameless furnace is made of carbon steel pipe with a diameter of 264 mm and a length of 600 mm. A special refractory was applied inside the chamber to maintain the temperature inside the furnace. After refractory installation, the inside diameter of the chamber was reduced to 150 mm. The inside temperature of the chamber is controlled by K-type thermocouples installed at the top of the furnace. The exhaust gases are conducted to a heat exchanger to preheat the inlet fresh air.
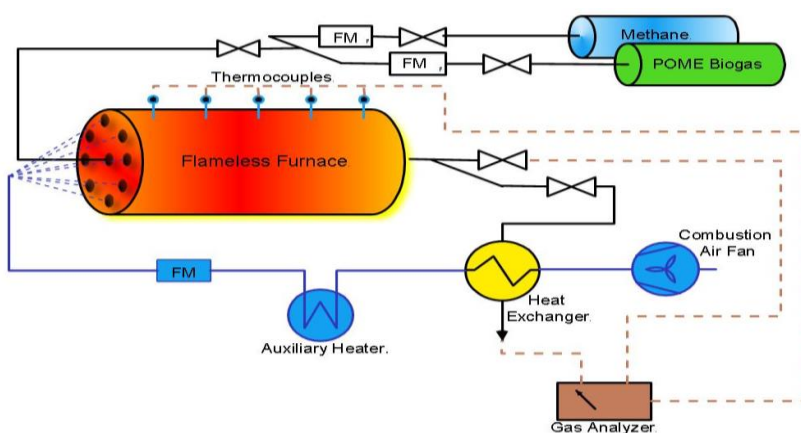

Fig. 1. Schematic of experimental set up

An electrical heater is projected to maintain the oxidizer temperature over the self-ignition temperature of palm oil mill effluent biogas. In one side of the chamber (burner zone), the central hole, the biogas inlet with a 5-mm diameter, is surrounded by the same size oxidizer inlets. The distance between fuel inlet jet and oxidizer inlet jet at the burner zone is 52.5 mm. At the other side (exhaust zone), a central hole with a diameter of 50 mm is provided for exhaust. The dual role burner is operated in traditional and flameless

combustion modes. In the first step (conventional combustion), the oxidizer and pure methane are mixed in the burner before injection and the reactant mixture is injected through the central nozzle (fuel nozzle). An electric spark igniter is employed in the conventional combustion mode for ignition. When the furnace heats up enough and the temperature is increased to more than 1200 K, a transition from traditional mode to flameless combustion begins. In this step, palm oil mill effluent biogas is utilized as the fuel and exhaust gases are conducted to the heat exchanger. The oxidizer was preheated at 900 K during the operation in flameless mode. Some measurement instruments, such as mass flow meters, pressure and temperature gages, and a gas analyzer, were employed to control and monitor the conditions of the system.

CFD Modeling

A CFD simulation was carried out in ANSYS 14; the ANSYS Modeler was used to model the flameless furnace, and ANSYS Meshing was used to mesh the chamber. Four sets of mesh were generated, and the number of nodes adopted was 90,280, 131,620, 162,230, and 195,700, respectively. For all generated meshes, the average of parameters such as temperature and concentrations of NO_x and CO were computed. It was observed that 195,700 nodes and 162,230 nodes produced almost identical results among average temperature (0.15% error) and CO and NO_x formation in the chamber. Hence, the case with 162,230 nodes was selected to reduce computing time.

All of the transport equations (continuity, energy, axial and radial momenta, radiative intensity, and turbulence kinetic energy and its dissipation rate) were solved using the commercial CFD package ANSYS FLUENT14 (Ansys, n.d.). All governing equations were solved using a second-order discretization scheme. To ensure the convergence of the solution, the residuals of the equations were set to drop below 10^{-4} for all variables, while for the energy equation, the residual was set at 10^{-6}. In steady-state conditions, the swirl velocity of components was neglected. To investigate various aspects of biogas flameless combustion, the simulation was performed with various fuel lean and stoichiometric conditions. The biogas flameless combustion characteristics were studied at various equivalence ratios ($\Phi = 0.5$, $\Phi = 1$) to compare the results with conventional combustion. The density of palm oil mill effluent biogas at 300 K is 0.9925 kg/m^3. The combustion reaction of the upgraded biogas consisting of 30% CO_2 and 70% CH_4 can be written as Eq. 1:

$$0.7CH_4 + 0.3CO_2 + 2(O_2 + 3.78N_2) \rightarrow CO_2 + 1.4H_2O + 5.292N_2 \qquad (1)$$
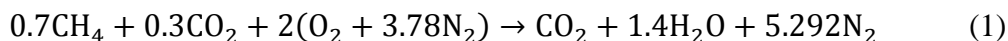
The standard k-ε formulation is considered for turbulent kinetic energy (k) and its dissipation (ε) because of its accuracy and robustness for wide range of turbulent flows. Because turbulent circumstances inside the chamber play a key role in flameless combustion formation, the k-ε model, which is valid for fully turbulent flows, can be effective in CFD modeling (Wilcox 1998). The thermal conductivity, specific heat, and viscosity were calculated with respect to the average species mass fraction. The momentum of the oxidizer at the inlet of the furnace is very high. Because radiation heat transfer in flameless combustion plays a crucial role in flameless combustion and pollutant formation reduction, radiation heat transfer between flameless combustor inner walls was taken into consideration in the simulation. A radiative transfer equation was solved for discrete solid angles across the numerical domain. Simulation of radiation heat transfer from various thicknesses was applied using the discrete ordinates (DO) model. At the internal walls,

***bioresources*.com**

non-slip and no species flux normal to the surfaces were considered. Both thermal heat transfer radiation and natural convection were considered for the heat loss calculation from combustor surfaces to the surroundings.

The Damköhler (D_a) number characterizes the behavior between mixing and reaction in a system by the ratio of a mixing, flow time-scale to a chemical time-scale (τ_f/τ_c) (Isaac *et al.* 2013). Large D_a values indicate mixing-controlled flames, and low D_a values indicate slow chemical reactions. EDM is usually applied when $D_a > 1$ (Ansys, n.d.). In this circumstance, because D_a is greater than one, the application of EDM has been reported to give acceptable results compared to other methods (Hosseini *et al*. 2014). Indeed, volumetric reaction-based with respect to two-step chemical kinetic mechanisms of biogas combustion is applied. In this method, combustion proceeds in the presence of the turbulence condition ($k/\varepsilon > 0$) and the application of an ignition source is not necessary to ignite the reactants. For NO_x formation, thermal NO_x formation is obtained *via* the extended Zeldovich mechanism with a steady-state assumption for the concentration of the free nitrogen atoms, and prompt NO_x constitution is evaluated using the reaction rate promulgated by De Soete (1975). The simple transport equation is considered for NO_x formation *via* the N_2O intermediate mechanism. A summary of boundary conditions of the simulation and settings are given in Tables 1 and 2, respectively.

Table 1. Boundary Conditions of Simulation

Oxidizer inlet	Temperature	uniform, 900 K
	Gauge Pressure	0
	Hydraulic diameter	5 mm
	Velocity	90 m/s
	Turbulent intensity	20
	Oxygen concentration	5 to 7%
	Density	0.383 g/L
	Mass flow rate	0.002699 to 0.002706 g/s
Fuel inlet	Temperature	uniform, 300 K
	Gauge Pressure	0
	Hydraulic diameter	5 mm
	Velocity	9 m/s
	Turbulent intensity	10
	Fuel ingredient	70% CH_4 30% CO_2
	Density	0.9925 g/L
	Mass flow rate	0.000175 g/s

Table 2. Settings of Simulation

Viscous model	*k-ε* Standard
Radiation model	DO
Combustion model	Species transport
Mixture properties	Methane-air 2-step
Turbulence chemistry interaction	EDM
Reaction	Volumetric
NO_x	Thermal NO_x Prompt NO_x N_2O-intermediate

RESULTS AND DISCUSSION

After the heat-up step, biogas from palm oil mill effluent was injected into the furnace as a fuel and preheated air with 5% and 7% volumetric oxygen concentration was charged as an oxidizer with dilution by pure nitrogen (N_2). Figure 2 depicts the configuration of the temperature in conventional methane combustion and palm oil mill effluent biogas flameless combustion with an oxygen concentration of 7%, $V_{inlet-oxidizer} = 90$ m/s, $T_{inlet-oxidizer} = 900, 1000, 1100, 1200$ K, and $\Phi = 0.5$. The enthalpy required to reach the ignition temperature of palm oil mill effluent biogas is supplied by the very high temperature oxidizer. In palm oil mill effluent biogas flameless combustion, the temperature of the furnace is more uniform compared to the conventional mode, and hot spots are removed. Because CO_2 forms around 30% of such biogas, the temperature of the reactants decreases because of the high heat capacity of CO_2, especially at high temperatures.
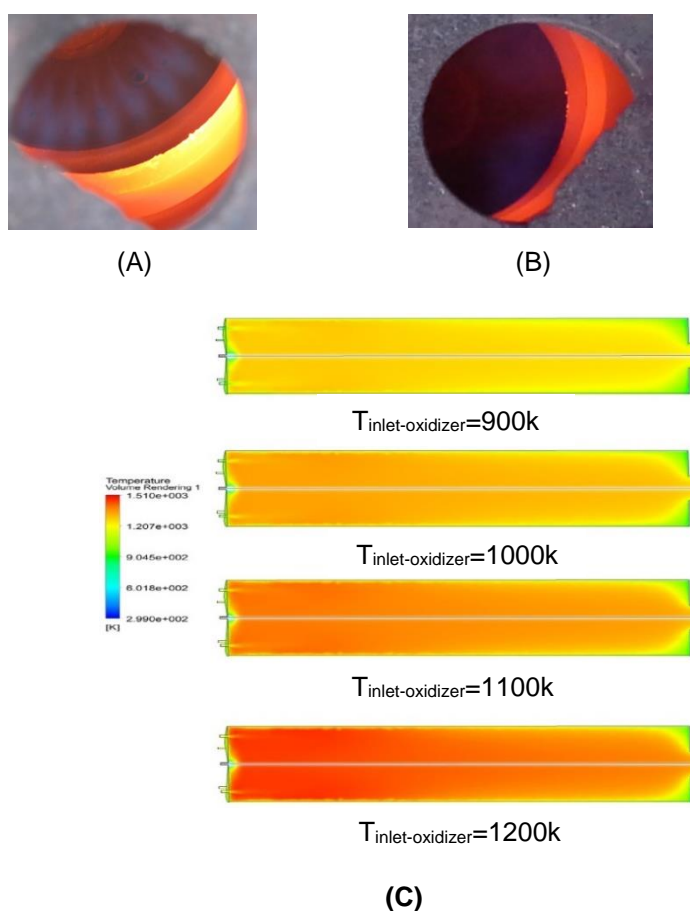

(A)   (B)

$T_{inlet-oxidizer}=900k$

$T_{inlet-oxidizer}=1000k$

$T_{inlet-oxidizer}=1100k$

$T_{inlet-oxidizer}=1200k$

(C)

Fig. 2. (A) Heating step (methane conventional combustion); (B) palm oil mill effluent biogas flameless combustion; (C) CFD simulation results

Temperature Uniformity and Flame Volume

Temperature uniformity inside the furnace is defined based on the normalized root mean square value calculated from all measured temperatures at various locations, as in Eq. 2 (Cho *et al.* 2013),

$$T_u = 1 - \sqrt{\frac{1}{N}\sum_{i=1}^{N}(\frac{T_i - \bar{T}}{\bar{T}})^2} \tag{2}$$

where T_u is the temperature uniformity inside the chamber, T_i is the measured temperature at the various locations (i), and $\bar{T}$ is the average of all measured temperatures at the various locations in the furnace. Figure 3 illustrates the location of installed thermocouples and measured temperature points inside the chamber in two dimensional scheme of furnace.
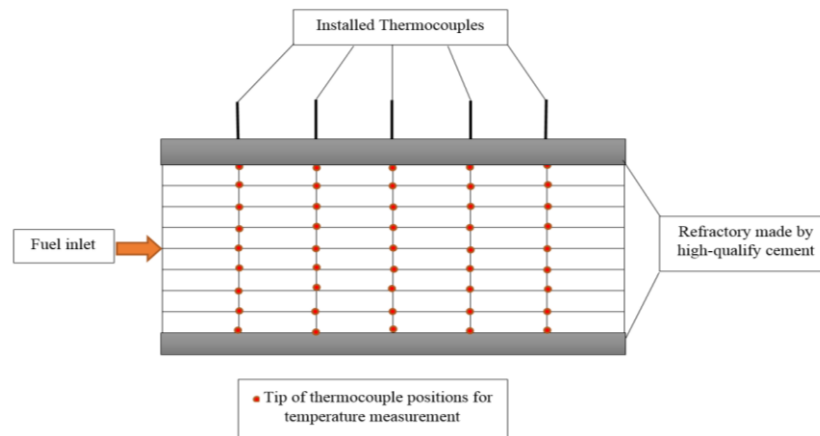
Fig. 3. Location of installed thermocouples and measured temperature points inside the chamber in two dimensional scheme of furnace

As one of the most important advantages of flameless combustion mode, the value of T_u approaches one in locations where a perfectly uniform temperature circumstance is observed in the furnace. Figure 4 shows the temperature uniformity inside the chamber in various cases investigated experimentally and numerically. The discrepancy between numerical results and experimental records could be attributed to the accuracy of the thermocouples, as well as various measurement techniques.
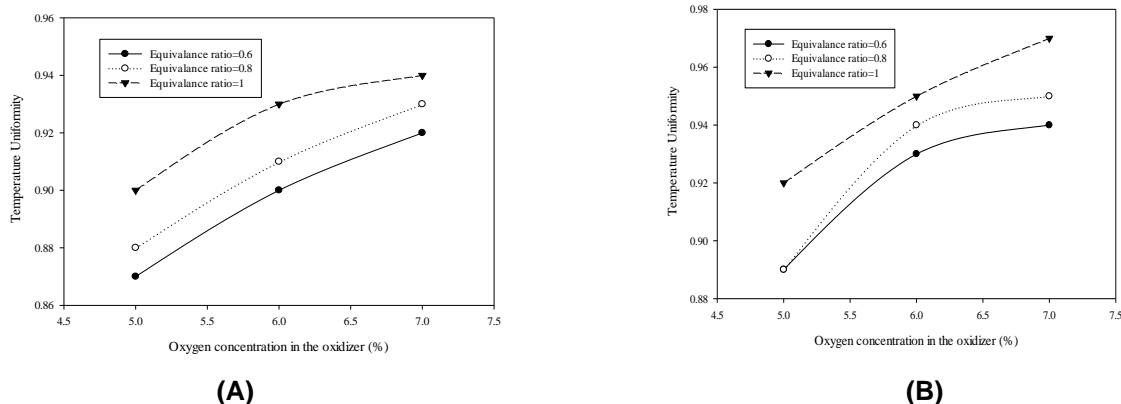
(A)   **(B)**

Fig. 4. Temperature uniformity inside the flameless chamber: (A) numerical results; (B) experimental results

The flame volume ratio (R_f) is defined as the nonvisible flame volume using the means of the oxidation mixture ratio (R_o). Some factors, such as the O_2 concentration in

the oxidizer, initial momentum of the fuel jet, and ratio of fuel inlet density to ambient gas density, have a great impact on the flame volume ratio,

$$R_f = \frac{V_f}{V_F} \qquad (3)$$

where R_f is the flame volume ratio, V_f is the flame volume, calculated based on the oxidation mixture ratio, and V_F is the volume of the combustion chamber (Yang and Blasiak 2006).

R_o is defined as the mass fraction of O_2 to the mass fraction of O_2 and the sum of O_2, which is required for complete combustion at each point of the combustor, as in Eq. 4 (Yang and Blasiak 2005).

$$R_o = \frac{m_o}{m_o + \sum_j S_j M_{F,j}} \qquad (4)$$

$$S = \frac{n_o M_o}{n_f M_f} \qquad (5)$$

where M is the molecular weight, m_o is the mass fraction of oxygen, and n is the stoichiometric coefficient, which for biogas stoichiometric combustion is determined from Eq. 1.

Based on the numerical results, the flame volume ratio for palm oil mill effluent flameless combustion mode is plotted in Fig. 5. To observe the volume of invisible flame in the flameless combustion mode, the contour of the temperature distribution inside the chamber is given in Fig. 4B. The oxygen concentration in the oxidizer plays a crucial role in the extension of non-luminous flame in the combustor. The maximum volume of non-luminous flame occurs under stoichiometric conditions when the concentration of oxygen in the oxidizer is 7%.

Thermal Efficiency

The specification of all bulks entering and leaving the boundary, such as fuel and oxidizer flow-rates and temperatures, were measured to quantify all energy states through the system. To solve the energy balance for the flameless furnace as an energy system, some assumptions are taken into consideration: (i) kinetic and potential energies are neglected; (ii) because the furnace is run for a relatively long time, $dE_{sys}/dt = 0$, (iii) palm oil mill effluent biogas and oxidizer are moisture-free and the reference temperature is T_R = 300 K, (iv) the lower heating value (LHV) of palm oil mill effluent biogas is the basis for calculations and the latent heat loss of vapor from exhaust is not considered, (v) Q_{sys} = $-Q_{sur}$. Based on Eq. 6, a plot of the efficiency of palm oil mill effluent biogas flameless combustion in various experimental conditions and numerical settings is presented in Fig. 6,

$$\eta = \left(1 - \frac{Q_{ex} + Q_s}{Q_f + Q_A}\right) \times 100 \qquad (6)$$

where (η) is combustion efficiency, (Q_{ex}) is the heat content of the flue gases, (Q_s) is energy loss from surface of the chamber, (Q_A) is thermal energy of the air, and (Q_F) is the fuel's heating value.

Both experimental and numerical results indicate that under stoichiometric conditions, when the concentration of oxygen in the oxidizer increases, the efficiency of palm oil mill effluent biogas flameless combustion also increases. The maximum

efficiency (approximately 61% in the experiment) is achieved when the percentage of oxygen in the oxidizer is 7%. The discrepancy between numerical results and experimental records could be attributed to the accuracy of measurement equipment.
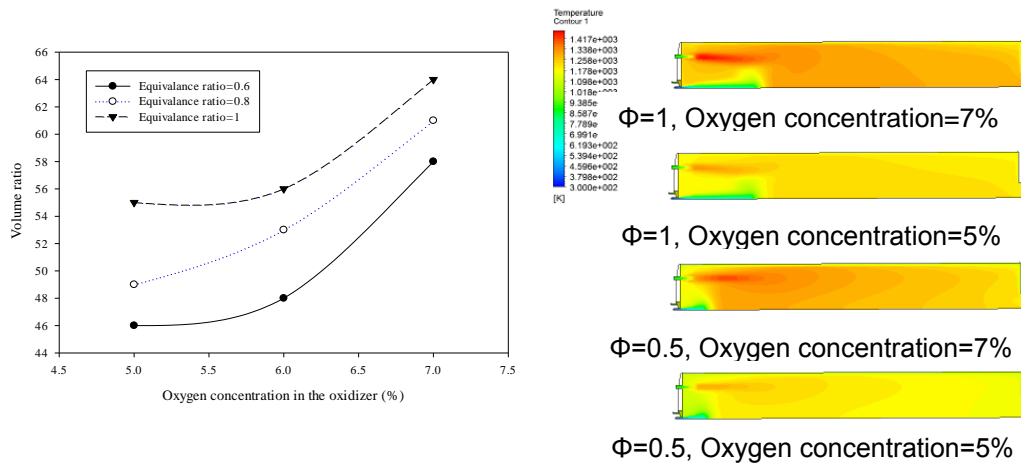

Fig. 5. (A) Flame volume ratio in palm oil mill effluent flameless combustion; (B) temperature distribution inside the chamber
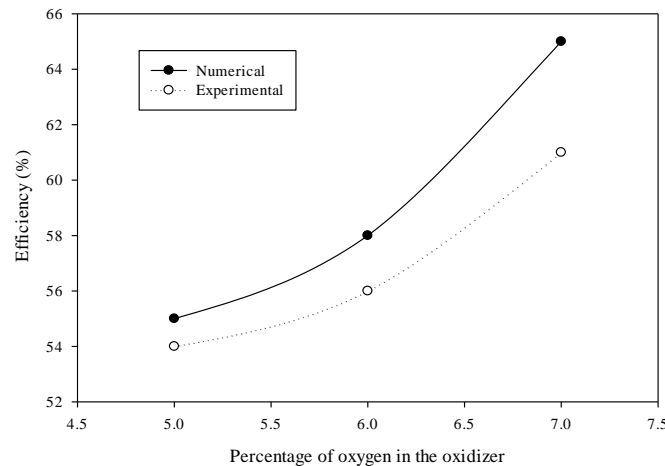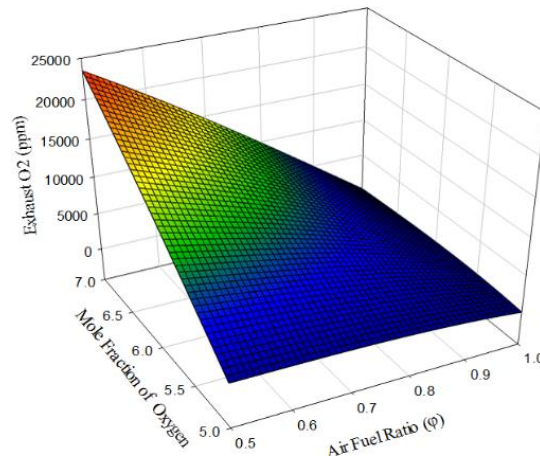

Fig. 6. Efficiency of palm oil mill effluent biogas flameless combustion ($\Phi = 1$)

Pollutants

In palm oil mill effluent biogas flameless combustion, the concentrations of CH_4 and CO_2 decrease more sharply along the furnace compared to traditional combustion. This means that the combustion phenomena occur homogeneously throughout the chamber in flameless mode. CO_2 and CH_4, as the biogas species, are lifted to the preheated oxidizer streamline as a result of various pressures. Because the velocity of the preheated diluted oxidizer is more than that of biogas, the vacuum causes the biogas species to be mixed with the oxidizer. Because of the turbulent circumstances, the mixing of the biogas and oxidizer species occurs immediately in flameless mode. This means a complete combustion occurs in the zone close to the burner. Figure 7 demonstrates the rate of oxygen (O_2) and CH_4 concentration in the exhaust gases with respect to various equivalence ratios and different dilution circumstances. The concentrations of O_2 in the exhaust gases of conventional

combustion and flameless mode were recorded at 118,240 and 23,400 ppm, respectively. Extremely low O_2 and CH_4 concentrations were recorded in highly diluted oxidizer in ultra-lean flameless combustion, reflecting complete combustion conditions.

(A)
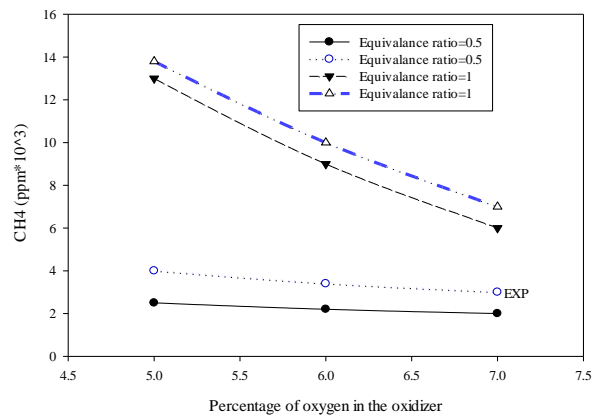
(B)

Fig. 7. (A) The rate of oxygen concentration in the exhaust gases; (B) CH_4 concentration in the exhaust gases

CO$_2$ and CO concentration in the exhaust gases are presented in Fig. 8 with respect to various percentages of dilution and different equivalence ratios.
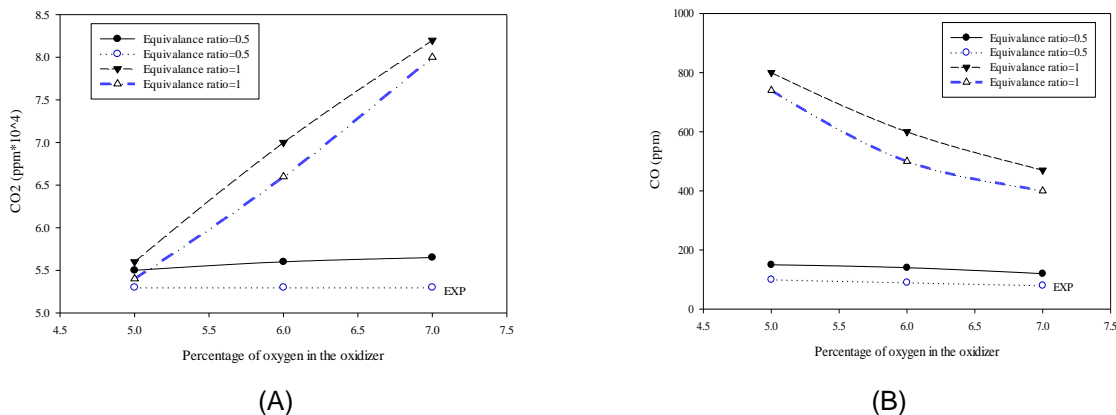
(A)   (B)

Fig. 8. (A) CO2 and (B) CO concentration in the exhaust of palm oil mill effluent biogas flameless combustion

When the rate of O_2 concentration in the preheated oxidizer increases, the rate of CO_2 formation intensifies (Wang *et al.* 2012). This means that, in the ultra-lean flameless mode, the concentration of CO_2 is very low. However, the concentration of CO recorded was higher than stoichiometric conditions (based on Eqs. 2 and 3).

In palm oil mill effluent biogas flameless combustion, the temperature inside the chamber is uniform (approximately 1200 K) and the hot spots are eliminated. On the other hand, flameless combustion takes place under ultra-lean circumstances. As a result, thermal NO_x and prompt NO_x are suppressed and the N_2O intermediate mechanism is responsible for NO_x formation in flameless mode. Figure 9 shows the numerical results of NO_x emission in biogas ultra-lean flameless combustion via various mechanisms.
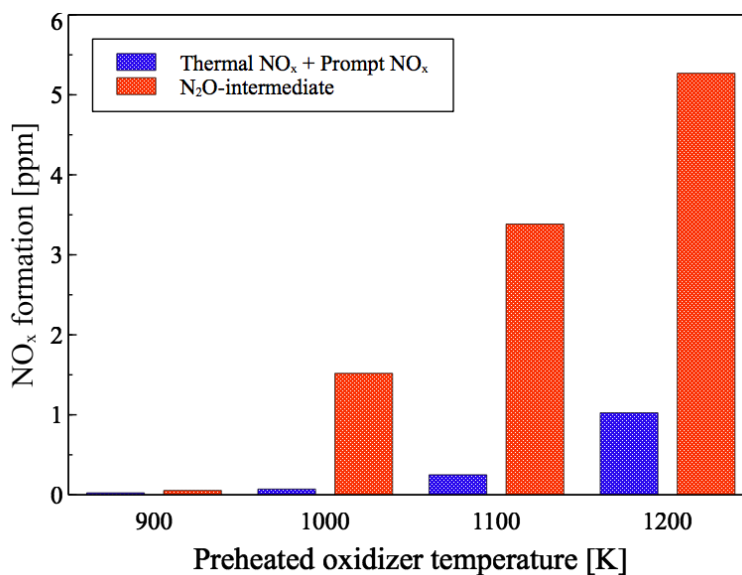

Fig. 9. NOx emission in palm oil mill effluent biogas flameless combustion

CONCLUSIONS

1. The feasibility of using palm oil mill effluent biogas in flameless combustion technology was investigated experimentally and numerically to propose a new method

for energy conversion of such biogas. In the biogas flameless combustion regime, the temperature inside the chamber is homogenous, hot spots are avoided, and pollutant emissions are very low. NO_x formation decreases in flameless mode because of the elimination of hot spots and low level of oxygen.

2. In palm oil mill effluent biogas flameless combustion, the biogas species are pulled to the streamline of the oxidizer because of various pressures. Higher heat capacity and better radiation heat transfer in the biogas flameless system are the consequences of large amounts of CO_2 species in the biogas flameless products.

3. The maximum temperature uniformity and non-luminous flame volume occur under stoichiometric conditions when the concentration of oxygen in the oxidizer is 7%. Under stoichiometric conditions, when the concentration of oxygen in the oxidizer increases, the efficiency of palm oil mill effluent biogas flameless combustion also increases. The maximum efficiency (approximately 61% in the experiment) was achieved when the percentage of oxygen in the oxidizer was 7%.

ACKNOWLEDGEMENT

REFERENCES CITED

Al-Juhaimi, F., Hamad, S., and Al-Ahaideb, I. (2014). "Biogas production through the anaerobic digestion of date palm tree wastes-process optimization," *BioResources* 9, 3323-3333. DOI: 10.15376/biores.9.2.3323-3333

Ansys, 14.0 Theory Guide. Fluent, Ansys, 14.0 Theory Guide, Ansys Inc 5 (2012).

Bedoya, I. D., Saxena, S., Cadavid, F. J., Dibble, R. W., Wissink, M. (2012). "Experimental study of biogas combustion in an HCCI engine for power generation with high indicated efficiency and ultra-low NOx emissions," *Energy Conversion and Management* 53, 154-162. DOI:10.1016/j.enconman.2011.08.016

Cho, E.-S., Shin, D., Lu, J., de Jong, W., and Roekaerts, D. J. E. M. (2013). "Configuration effects of natural gas fired multi-pair regenerative burners in a flameless oxidation furnace on efficiency and emissions," *Applied Energy* 107, 25-32. DOI:10.1016/j.apenergy.2013.01.035

De Soete, G. G. (1975). "Overall reaction rates of NO and N_2 formation from fuel nitrogen," Symposium (International) on Combustion 15, 1093-1102. DOI: 10.1016/S0082-0784(75)80374-2

Dungani, R., Jawaid, M., Khalil, H. P. S. A., and Aprilia, S. (2013). "A review on quality enhancement of oil palm trunk," *BioResources* 8, 3136-3156. DOI: 10.15376/biores.8.2.3136-3156

Gassoumi, T., Guedri, K., and Said, R. (2009). "Numerical study of the swirl effect on a coaxial jet combustor flame including radiative heat transfer. Numerical heat transfer, Part A: Applications 56, 897-913. DOI:10.1080/10407780903466535

Hansen, S. B., Olsen, S. I., and Ujang, Z. (2012). "Greenhouse gas reductions through enhanced use of residues in the life cycle of Malaysian palm oil derived biodiesel," *Bioresource Technology* 104, 358-366. DOI: 10.1016/j.biortech.2011.10.069

Hosseini, S. E., and Abdul Wahid, M. (2015). "Pollutant in palm oil production process," *Journal of the Air & Waste Management Association* 65, 773-781. DOI:10.1080/10962247.2013.873092

Hosseini, S. E., Bagheri, G., and Wahid, M. A. (2014). "Numerical investigation of biogas flameless combustion," *Energy Conversion and Management* 81, 41-50. DOI: 10.1016/j.enconman.2014.02.006

Hosseini, S. E., and Wahid, M. A. (2013). "Feasibility study of biogas production and utilization as a source of renewable energy in Malaysia," *Renewable and Sustainable Energy Reviews* 19, 454-462. DOI:10.1016/j.rser.2012.11.008

Isaac, B. J., Parente, A., Galletti, C., Thornock, J. N., Smith, P. J., and Tognotti, L. (2013). "A Novel methodology for chemical time scale evaluation with detailed chemical reaction kinetics," *Energy & Fuels* 27, 2255-2265. DOI:10.1021/ef301961x

Rebola, A., Coelho, P. J., and Costa, M. (2013). "Assessment of the performance of several turbulence and combustion models in the numerical simulation of a flameless combustor," *Combustion Science and Technology* 185, 600-626. DOI:10.1080/00102202.2012.739222

Wang, L., Liu, Z., Chen, S., and Zheng, C. (2012). "Comparison of different global combustion mechanisms under hot and diluted oxidation conditions," *Combustion Science and Technology* 184, 259-276. DOI:10.1080/00102202.2011.635612

Wilcox, D. C. (1998). "Turbulence modeling for CFD," La Canada, CA: DCW industries, 2, 103-217.

Yang, W., and Blasiak, W. (2005). "Numerical study of fuel temperature influence on single gas jet combustion in highly preheated and oxygen deficient air," *Energy* 30, 385-398. DOI:10.1016/j.energy.2004.05.011

Yang, W., and Blasiak, W. (2006). "CFD as applied to high temperature air combustion in industries furnaces," *IRFR Combustion Journal*.